Monitoring Expression and Clustering of the Ionotropic $5HT_3$ Receptor in Plasma Membranes of Live Biological Cells†

Horst Pick, Axel K. Preuss,‡ Michael Mayer,§ Thorsten Wohland,|| Ruud Hovius, and Horst Vogel*

Institute of Biomolecular Sciences, Swiss Federal Institute of Technology, Lausanne, CH-1015 Lausanne, Switzerland

Received August 6, 2002; Revised Manuscript Received November 28, 2002

ABSTRACT: The ionotropic $5HT_3$ receptor was expressed in transiently transfected mammalian cells, yielding an unprecedented high concentration of up to 12 million receptors per cell. Receptor traffic in the plasma membrane of live cells was observed continuously over 24 h by fluorescence scanning confocal microscopy. This was possible by using $5HT_3$ receptor-specific fluorescent ligands with high binding affinity and low off-rate to pulse label receptors at any time after appearance on the cell surface, and label subsequently those receptors expressed later by another, spectrally distinguishable, high-affinity fluorescent ligand. Having reached a critical cell surface concentration of ∼3000 receptors/μm^2, the receptors started to aggregate in patches with a 4-fold increased surface concentration. The clusters were constantly delivered from a pool of freshly expressed receptors isotropically distributed within the basolateral region of the cell membrane. From there, they migrated to and accumulated on the apical cell surface ∼9 h after transfection. Individual clusters grew until they reached a critical size of 1−2 μm when they merged to form with 3−5 μm large macroclusters. Clustered receptors were immobile on the minute time scale but always coexisted with monomeric receptors in the regions surrounding the clusters as revealed by fluorescence correlation spectroscopy. Because the receptor density of 12 000 receptors/μm^2 in the patches is as high as that found in two-dimensional crystals of certain membrane proteins, such patches might be a proper source for direct crystallization of membrane proteins without prior purification.

High-level expression of cell surface receptors is important for structural and functional characterization of receptor proteins. Plasma membranes comprising the receptors of interest at high density are a prerequisite to be used directly or for purifying such membrane proteins in milligram quantities for structural investigations by electron (*1*−*3*) or X-ray diffraction (*4*), scanning probe techniques (*5*), and NMR spectroscopy (*6*).

Such high receptor densities are only in rare cases directly available from natural sources. A classical example is the nicotinic acetylcholine receptor (nAchR) which in certain neuromuscular junctions as well as in the electric organ of *Torpedo marmorata* (*7*, *8*) exists in a high-density packed state of ∼10 000 receptors/μm^2 (*9*). Bacteriorhodopsin is another membrane protein found in a quasi-two-dimensional crystalline form in native purple membranes of *Halobacterium salinarium* (*10*−*12*). In both cases, reasonably good two-dimensional crystals were obtained directly from natural membranes without protein purification, delivering molecular details of the three-dimensional structures of the two proteins (*13*−*15*). Another remarkable example is the photoreceptor rhodopsin. In the bovine rod outer segments, the photoreceptor density is so high that the disk membranes of the rods can be used directly to solubilize and crystallize rhodopsin without further purification (*16*).

With the help of recombinant DNA technology, nearly any membrane receptor protein can be expressed in heterologous systems, and some receptors have been shown to be expressed in large amounts (*17*−*19*). We are interested in developing general strategies for controlling the receptor density and finally reaching the maximal possible cell surface concentration of ∼10 000 receptors/μm^2 suited to appling the aforementioned strategies for direct two- or three-dimensional crystallization. An important step in reaching this goal is understanding the mechanism of how membrane proteins cluster to such high densities.

In the work presented here, we monitor for the first time a recombinantly expressed cell surface receptor, the short splicing variant of the ligand-gated ion channel 5-hydroxytryptamine receptor of class 3A ($5HT_3R$) (*20*), in vivo and continuously during the course of its expression, i.e., from its first appearance on the cell surface, during the increase of its surface concentration, and until its final clustering in defined membrane patches. The receptors were detected as fluorescent ligand−receptor complexes by confocal microscopy using recently developed $5HT_3R$-specific, high affinity fluorescent ligands (*21*, *22*). These ligands show a low off-rate such that the ligand−receptor complexes remain stable during the whole time period of the experiment (*23*). As a

† This work was financially supported by the Swiss National Science Foundation and EPFL Grant no. 581.448.

* To whom correspondence should be addressed: EPFL-LCPPM, CH-1015 Lausanne, Switzerland. E-mail: horst.vogel@epfl.ch.

‡ Present address: Department of Physiology and Biophysics, Mount Sinai School of Medicine of New York University, 1425 Madison Ave., New York, NY 10029.

§ Present address: Department of Chemistry and Chemical Biology, Harvard University, 12 Oxford St. (box 53), Cambridge, MA 02138.

|| Present address: Department of Chemistry, Mudd Bldg., Room 239, Stanford University, Stanford, CA 94305-5080.

10.1021/bi026576d CCC: $25.00
Published on Web 01/10/2003

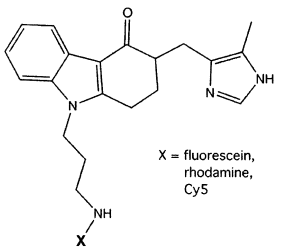

FIGURE 1: Chemical structure of the ligands that were used. The $5HT_3R$-specific antagonist GR119566 (X = H or GR-H) was labeled at X with fluorescein, rhodamine B, and Cy5, yielding GR-flu, GR-rho, and GR-Cy5, respectively.

central strategy of this work, various fluorescent ligands (Figure 1), each carrying a spectroscopically distinguishable chromophore attached to the same pharmacophore, were bound consecutively to $5HT_3Rs$ on HEK293 cells; thereby, it was possible to observe the appearance of receptors during their expression and distinguish those which appeared at different times on the cell surface. This novel approach reported here is suited to following the assembly and turnover of membrane receptor proteins in general.

We have chosen to investigate the 5-HT_3R because it is well-characterized pharmacologically, biochemically, and biophysically, in particular with fluorescent ligands (*22*−*26*). Together with the nicotinic acetylcholine, the GABA, and the glycine receptors, the $5HT_3R$ is a member of a superfamily of multimeric ligand-gated ion channels (*20*, *27*, *28*). In contrast to its heteromeric relatives, it is composed of five identical subunits with an estimated relative molecular mass of 270 kDa (*20*, *29*). According to the distribution of hydrophilic and hydrophobic amino acids within the protein sequence, each subunit of the 5-HT_3R is predicted to traverse the membrane four times (*20*). Therefore, the receptor densities in the observed receptor clusters have to be compared with those in the naturally occurring clusters of the nAchR (*9*, *14*, *15*).

MATERIALS AND METHODS

Plasmid Construction. For cloning and heterologous expression of the receptor, we used the full-length coding region of the murine $5HT_3R$ provided by K. Lundstrom (Research Laboratories, F. Hoffman-La Roche, Basel, Switzerland). The corresponding cDNA was subcloned as a 1.5 kb *Sma*I−*Not*I DNA fragment into the mammalian expression vector CMV_β (CLONTECH, Palo Alto, CA) by replacing the original β-galactosidase reporter gene. In this construct, $5HT_3R$ expression is under the control of the human cytomegalovirus immediate early gene promoter. All subcloning steps were controlled by restriction pattern analysis. The final construct was verified through sequence analysis.

Cell Lines and Cell Culture. Human embryonic kidney (HEK293) cells were grown in DMEM/F12 (Dulbecco's modified Eagle's medium, GIBCO BRL, Rockville, MD). The medium was supplemented with 2.2% (v/v) fetal calf serum (GIBCO BRL). The cultures were kept in the incubator (37 °C and 5% CO_2) and were split in regular time intervals.

Transient Transfection of Cells. Sixteen to twenty hours before transfection, exponentially growing cells were seeded (10^5 cells/mL) on sterile microscope cover slides placed in a six-well plate. The cells were transfected using calcium phosphate-precipitated DNA (*30*). Five hundred microliters of a 250 mM $CaCl_2$ solution containing 25 μg of plasmid DNA was added to an equal volume of a solution containing 140 mM NaCl, 1.4 mM Na_2HPO_4, and 50 mM HEPES (pH 7.05) at 23 °C. One minute after the two solutions had been mixed at room temperature, this transfection mixture was added to the cell culture medium. For each milliliter of cell medium, 100 μL of calcium phosphate−DNA precipitate (containing 2.5 μg of plasmid DNA) was added. After 4 h at 37 °C in the incubator, the transfection medium was replaced with fresh medium.

Radioligand Binding Assays. Membrane preparations of 10^6 cells were incubated for 60 min at room temperature in a solution of 1 mL of 10 mM HEPES (pH 7.4) and 0.8 nM 3-(5-methyl-1*H*-imidazol-4-yl)-1-(1-[^{3}H]methyl-1*H*-indol-3-yl)propanone ([^{3}H]GR65630, 61 Ci/mmol, NEN-DuPont, Boston, MA). The incubation was terminated by rapid filtration [Whatman GF/B filters presoaked for 15 min in 0.5% (w/v) polyethylenimine] followed by two washings with 3 mL of ice-cold 10 mM HEPES (pH 7.4). Filters were transferred to scintillation vials containing 4 mL of Ultima Gold TM (Packard, Meriden, CT). The amount of radioactivity was measured in a Tri-Carb 2200CA liquid scintillation counter (Packard) and corrected for quenching and counting efficiency. The total number of ligand binding sites was determined at six different concentrations of [^{3}H]GR65630. The level of nonspecific binding was determined in the presence of 1 mM quipazine (Tocris-Cook-son, Bristol, U.K.). All experiments were performed in triplicate. The total number of binding sites was evaluated from binding isotherms obtained from experimental data by curve fitting using an iterative Levenberg−Marquardt algorithm (Igor, WaveMetrics Inc., Lake Oswego, OR).

Fluorescent Ligands. The antagonist GR-H (GR119566) was labeled with either fluorescein 5-isothiocyanate (Molecular Probes, Eugene, OR), rhodamine B isothiocyanate (Fluka, Buchs, Switzerland), or Cy5 succinimide (Amersham, Zürich, Switzerland) as described elsewhere (*21*, *22*). The fluorescent ligands are termed GR-flu, GR-rho, and GR-Cy5, respectively (Figure 1).

Laser Scanning Fluorescence Microscopy. A Zeiss LSM510 laser scanning confocal microscope was used (Zeiss, Oberkochen, Germany). Cells grown in DMEM/F12 medium on 0.18 mm thick glass cover slides were transferred to a perfusion chamber and analyzed either in the cell growth medium or in PBS buffer. Detection of and distinction between fluorescence signals of rhodamine (excitation at 543 nm) and fluorescein (excitation at 488 nm) were achieved by using appropriate filters (Zeiss filter set numbers 10 and 15). To further minimize cross talk between the channels, the excitation wavelength alternated between each scan while the image was being recorded. Scanning speed and laser intensity were adjusted to avoid photobleaching of the fluorescent probes and damage or morphological changes to the cells. Images of the top surface of a cell were reconstructed from a stack of 0.3 μm thick optical sections using Zeiss LSM software. Areas of receptor clusters were evaluated using Zeiss LSM software.

Quantification of Fluorescence Intensities in Confocal Microscopy. The concentrations of $5HT_3R$−ligand complexes on the surface of cell membranes were estimated by

comparing fluorescence intensities of confocal micrographs of cells, for instance, in receptor cluster regions with those of giant (>10 μm in diameter) unilamellar vesicles comprising a defined amount of rhodamine-labeled lipids (*31*). The lipid mixture was composed of 67−70% asolectin (Fluka), 25% 1-palmitoyl-2-oleoyl-*sn*-glycero-3-[phospho-*rac*-(1-glycerol)] (POPG), (Avanti Polar Lipids, Alabaster, AL), 5% cholesterol (Sigma, Buchs, Switzerland), and 0.2−3.3% rhodamine B isothiocyanate-labeled 1-palmitoyl-2-oleoyl-*sn*-glycero-3-phosphoethanolamine. The fluorescent lipid was synthesized by standard procedures in our laboratory.

Fluorescence Correlation Spectroscopy (FCS). A home-built FCS instrument as described in detail elsewhere (*22*) was used. Cy5 was excited at 633 nm by a helium−neon (HeNe) laser (Melles Griot, Irvine, CA) delivering a beam diameter of 1 mm. The cross section of the laser beam was expanded by a factor of 3 using a Keplerian beam expansion. The laser beam was then reflected by a dichroic mirror (for Cy5, 645DRLP02, Omega, Brattleboro, VT) and coupled into the microscope objective. The beam expansion ensured that a large portion of the microscope objective back aperture (63× water-immersion C-Apochromat, NA = 1.2, Zeiss) was illuminated. The fluorescent light of the sample was collected by the same objective and, after traversing an optical band-pass filter (for Cy5, 670DF40, Omega), focused to an avalanche photodiode (SPCM 100, EG&G, Princeton, NJ). The power of the laser beam entering the microscope was set to 0.7 mW for the HeNe laser. This power level created sufficiently high fluorescence signals per molecule, but was still low enough to keep the amount of photobleaching negligible.

FCS measurements were performed at 35 °C on HEK293 cells in PBS buffer 24 h post-transfection. Cells expressing $5HT_3$Rs were labeled with a fluorescent ligand by incubation in a solution of 12 nM GR-Cy5 in bulk. Experimental autocorrelation functions (ACFs) of GR-Cy5 bound to HEK293 cells were evaluated by using a model with three components: the free ligand in aqueous solution, the free ligand partitioned into the cell membrane, and the receptor-bound ligand (*24*).

RESULTS AND DISCUSSION

Efficiency of Receptor Expression. The number of receptors on the cell membranes was monitored for a period of 24 h after transfection by assessing the binding of the $5HT_3$R-specific radioactive ligand [^{3}H]GR65630 to the cells. In that period, the receptor number steadily increased until it reached a maximal value at 24 h (Figure 2). Ligand binding experiments performed on samples 24 h after transfection showed that the amount of membrane-bound radioligand as a function of the concentration of free ligand was fitted well by a Langmuir binding isotherm (Figure 2). Specific binding corresponding to the presence of 1.25×10^7 receptors per cell was observed, taking into account that in this particular case only 80% of the total number of cells were transfected as seen by confocal fluorescence microscopy (see below).

Clustering of Receptors. GR-rho and GR-flu (Figure 1) were used to monitor recombinant $5HT_3$Rs on the plasma membrane of live cells in the form of ligand−receptor complexes by confocal fluorescence microscopy. These two ligands have previously been shown to bind selectively with

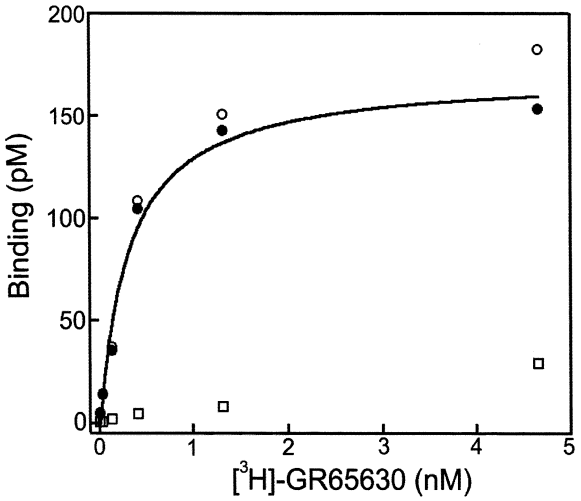

FIGURE 2: Binding of the radioactive ligand [^{3}H]GR65630 to plasma membranes of HEK293 cells 24 h after transfection with $5HT_3$R plasmid DNA. The level of specific binding (●) was calculated as the difference between the levels of total (○) and nonspecific (□) binding. Fitting the specific binding data with a Langmuir isotherm (solid line) yielded a dissociation constant K_d of 0.4 nM and a total amount of 150 pM binding sites corresponding to an average number of 1.25×10^7 functionally active receptors per transfected cell.

similar high affinity to $5HT_3$Rs both purified and recombinantly expressed on the plasma membrane of HEK293 cells (*22*−*25*). Here, we found that GR-rho, in contrast to GR-flu, could not be removed from the $5HT_3$R binding site, even when cells were washed extensively with pure buffer solution.

The confocal micrograph in Figure 3 shows a live HEK293 cell, which was incubated in a 2 nM solution of GR-flu 24 h after transfection with $5HT_3$R DNA. Bright green fluorescent patches distributed over the cell surface were observed. These fluorescent features are due to complexes formed between GR-flu and $5HT_3$Rs; they were absent, if the cells were preincubated with quipazine, a nonfluorescent ligand, which is known to compete with GR-flu for binding to the 5-HT_3R (*23*). HEK cells stained with GR-flu 24 h after transfection show 30−50% of the cell surface covered by fluorescent $5HT_3$R clusters.

Estimation of Receptor Densities in Clusters. To evaluate the surface area of HEK cells, we treated cells with a solution of 300 μM EGTA whereby they adopted a nearly perfect spherical shape. The diameters of the spherical cells were determined by confocal microscopy to be 27 ± 3 μm. Because 24 h after transfection 1.25×10^7 receptors (as determined by radioligand binding assays) are distributed over 1150 μm^2, i.e., over half of the cell surface, we estimate a density of 11 000 receptors/μm^2 (range according to the uncertainty of cell size, 9 000−14 000 per μm^2) in the patches.

In addition, for cells 24 h post-transfection, we determined a density of ∼13 000 receptors/μm^2 from the fluorescence intensities of the patches by comparison with reference fluorescent lipid membranes of giant unilamellar vesicles. This value is very close to the values estimated from radioligand binding assays.

The fluorescence-based determination of receptor densities is fast and reliable. We have bound mixtures of varying proportions of Cy5 and rhodamine-labeled fluorescent ligands.

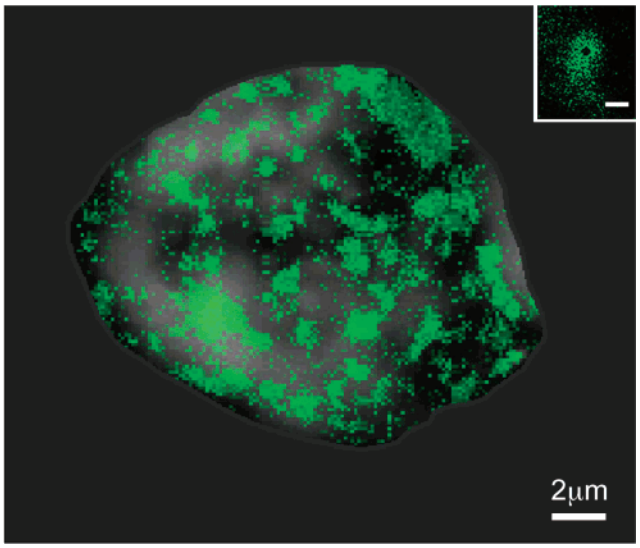

FIGURE 3: Image of a live HEK293 cell transiently expressing $5HT_3$Rs, 24 h after transfection. The receptors appeared as clusters at the cell surface, visualized after selectively binding GR-flu from a 2 nM solution. The final image of the cell is composed of 50 individual confocal microscopic planar cross-section images taken consecutively at 0.3 μm height steps. In the inset, a high-intensity laser pulse (488 nm, 3.75 mW, 3 s) was used to bleach a ca. 0.3 μm diameter spot into the core of a fluorescent receptor cluster shown at the upper right corner (scale bar is 1 μm). The fluorescence intensity of the membrane-bound GR-flu in the bleached spot measured with a low intensity probe beam was ~20% of the original intensity before bleaching, and remained constant at this low level for more than 15 min.

These two chromophores are capable of performing fluorescence resonance energy transfer (FRET) from rhodamine as a donor to Cy5 as an acceptor. The fact that we never saw FRET under different proportions of rhodamine to Cy5-labeled receptors indicates that in the patches the distance between two fluorescent labeled ligands is on average >8 nm.

Our approach to measuring receptor densities is novel, can be used for monitoring continuously and in situ the appearance of functional receptors in live cells, and is therefore much more reliable than any other labeling methods such as antibody staining or gold labeling with subsequent analysis by electron microscopy.

Dynamics of Receptor Distribution on Cell Surfaces. The slow off-rate of GR-rho from the ligand−receptor complex makes it possible to monitor the distribution of $5HT_3$Rs in the plasma membrane over time.

In a first series of experiments, HEK293 cells were stained at different times after transfection with GR-rho. Five to six hours after transfection, the first receptors appeared to be almost homogeneously distributed in the form of a faintly stained ring at the basolateral region of the cell (Figure 4A). Cells stained 8−11 h after transfection showed, in addition to the ring-like receptor distribution, fluorescent receptor clusters, first slightly above the ring but later more and more toward the top of the cell (with respect to the supporting glass slide).

To distinguish between receptors expressed at different times on the cell surface, we first stained cells 5 h after transfection with GR-rho and restained these cells 1, 2, 4, and 6 h later with GR-flu. Representative examples are depicted in Figure 4B−D. Figure 4B shows a cell which was stained 5 h after transfection with GR-rho but observed only 9 h after transfection (i.e., 4 h after the staining). Directly after the confocal micrograph had been recorded, the cell was restained with GR-flu and the micrograph recorded a few minutes later delivering the images shown in panels C and D of Figure 4. The newly expressed receptors in the basolateral region (stained with GR-flu) could easily be distinguished from the earlier expressed receptors (stained with GR-rho) at the cell center due to the spectrally different labels.

Double staining experiments also gave insight into the process of receptor cluster formation. Figure 4D shows a GR-rho-labeled receptor cluster surrounded by freshly formed GR-flu-labeled receptors in the basolateral ring. Outside of the basolateral ring, receptor clusters are found composed of a GR-rho-labeled core and a GR-flu-labeled periphery.

During the experiments documented in Figure 4, the fluorescent ligands were bound to and remained on the 5-HT_3R over a long period on the cell membrane. It is known from other ligand-gated ion channels and also from G protein-coupled receptors that receptors might be internalized upon agonist binding (*32*, *33*). To demonstrate that this did not occur upon antagonist binding in our present case, we performed a series of control experiments by first binding a fluorescent ligand to the cell surface 5-HT_3Rs which was then replaced with another one after different periods of incubation. The results, documented as Supporting Information, clearly demonstrate that the 5-HT_3Rs are not internalized but remain on the cell surface in the original orientation under our experimental conditions.

Figure 5 depicts the evolution of the receptor distribution from a homogeneous nonclustered basolateral ring (cells ≤8 h post-transfection) to the formation of receptor clusters (cells ≥9 h post-transfection). Fluorescence intensities are normalized per square micrometer. The maximal fluorescence signal of 100 indicates 13 000 receptors/μm^2. The correlation between fluorescence intensity and receptor density is linear within this region of interest. The homogeneously distributed receptors in the basolateral ring were first detected in cells 5 h after transfection and showed a density of ~1 000 receptors/μm^2. The receptor density increased in this homogeneous region linearly with time, reaching a value of ~3 000−4 000 receptors/μm^2 in cells 7−8 h after transfection. Then in cells 9 h after transfection, the first clusters appeared where the density increased substantially to ~9 000 receptors/μm^2. The receptor density in the clusters increased further until it reached a limiting value of ~13 000 receptors/μm^2 in cells 14−15 h after transfection.

A detailed analysis of $5HT_3$R clusters revealed a large variability of shapes and sizes.

The size of the clusters increased continuously with time. Nine hours after transfection, the most frequent cluster size was between 0.75 and 1 μm in diameter. A few clusters were up to 2 μm. Twenty-four hours after transfection, clusters appeared from ~0.5 μm in diameter to larger round or elongated patches up to 5 μm in size, and the most frequent diameter was 1−2 μm. While the fluorescence intensity distribution in the smaller clusters was in general homogeneous, some larger clusters (>3 μm) showed more than one fluorescent spot, as if they were formed from the merger of several smaller clusters. The histogram in Figure 5 (inset)

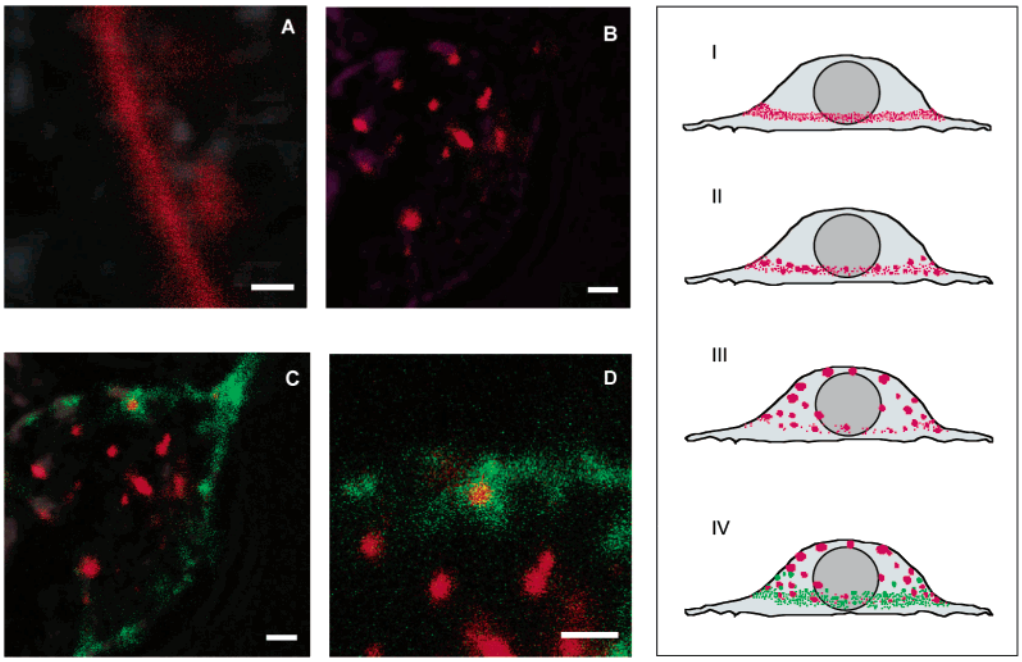

FIGURE 4: Distribution of $5HT_3$Rs on the surface of HEK293 cells during transient expression. Panels A−D are confocal micrographs showing the distribution of receptors stained with fluorescent ligands at different times after transfection. The bar in panel A corresponds to 1 μm and that in panels B and C to 2 μm; panel D is a 2-fold enlarged view of a particular region of panel C. (A) The cell was stained with a 5 min pulse in a 2 nM GR-rho solution 5 h after transfection, washed, and measured a few minutes later. (B) The cell was pulse labeled with GR-rho 5 h after transfection but recorded only 9 h after transfection (i.e., 4 h after labeling with GR-rho). (C and D) After the micrograph shown in panel B had been recorded, the same cell was restained with GR-flu (i.e., 9 h after transfection) and imaged just after the second labeling; green are GR-flu-labeled and red GR-rho-labeled receptors. The panel on the right shows schematically the contours of a cell comprising a circular nucleus in the center and the receptor distribution as either small red points (I) or clusters (II−IV) at four different stages after transfection. Scheme I corresponds to micrograph A. Scheme II indicates the transition from a homogeneous distribution in the basolateral ring to the beginning of receptor aggregation. Scheme III corresponds to micrograph B showing the clusters distributed at the apical cell surface areas. Scheme IV summarizes the observations of micrographs C and D showing large apical red clusters together with newly formed receptors in the basolateral ring represented by green dots.

shows the percentage of which the different cluster sizes covered the total cell surface; clusters on 20 different cells 9 and 24 h after transfection were evaluated.

Receptor Mobility. Twenty-four hours after transfection, shapes and the distribution of receptor clusters did not change significantly over 1 h. At this stage of the transient expression process, we investigated the lateral mobility of the receptors by photobleaching experiments and FCS.

Cells were first stained for 2 min in culture medium containing 2 nM GR-flu and then washed with a medium free of fluorescent ligands. After a particular GR-flu-labeled receptor cluster had been localized on the cell surface by confocal microscopy, a 0.3 μm diameter spot was bleached into the center of the fluorescent cluster (inset of Figure 3). Approximately 20% of the original GR-flu fluorescence intensity remained in the bleached area as determined by the low-power probe beam of the laser scanning confocal microscope. Similar experiments were carried out with cells stained with GR-rho where the fluorescence intensity in the bleached spot did not change over a time period of 15 min, indicating that a large portion of the receptors is immobile over that time period.

To yield further insight into receptor mobility, FCS measurements were performed on cell surfaces. FCS is a versatile technique for obtaining information about the dynamics of molecular interactions (*34*−*36*). Cells were stained with GR-Cy5 because this fluorescent ligand exhibits high photostability and its emission is in a wavelength range with low cellular autofluorescence (*23*). Scanning the cell surface by FCS revealed two major $5HT_3$R populations. At certain regions on the cell surface, fluorescence intensity fluctuations such as those shown in Figure 6A were measured; the corresponding autocorrelation functions (ACFs) were best fitted by three correlation times (*24*) corresponding to the diffusion of free GR-Cy5 ligands in solution ($\tau_1 <$ 0.3 ms, $D = 10^{7}-10^{-6}$ cm^2/s), ligands partitioned into the cellular membrane ($\tau_2 = 1-10$ ms, $D = 10^{-9}-10^{-8}$ cm^2/s), and ligands bound to nonclustered receptors in the cellular membrane ($\tau_3 > 20$ ms, $D = 10^{-10}-10^{-9}$ cm^2/s). In other regions on the cell surface, fluorescence signals much higher in intensity as before were observed, the magnitudes of which, however, decreased within seconds due to photobleaching (Figure 6B). The fluorescence decay could be fitted by two exponentials with time constants of 0.5 and 3.4 s. The amplitude of the fast component was at least 6 times higher than that of the slower component. The presence of two time constants indicates that the fluorescent ligand probes two different environments on the cell surface. After the two-exponential fit had been subtracted from the experimental photobleaching decay, a flat residual trace was obtained comprising random fluctuating fluorescent signals (Figure 6C), similar to that observed for single receptor proteins diffusing laterally in the membrane plane. This shows that the major part of the $5HT_3$Rs in these regions is immobile on the minute time scale and a minor fraction shows lateral mobility. We assume that such regions correspond to the

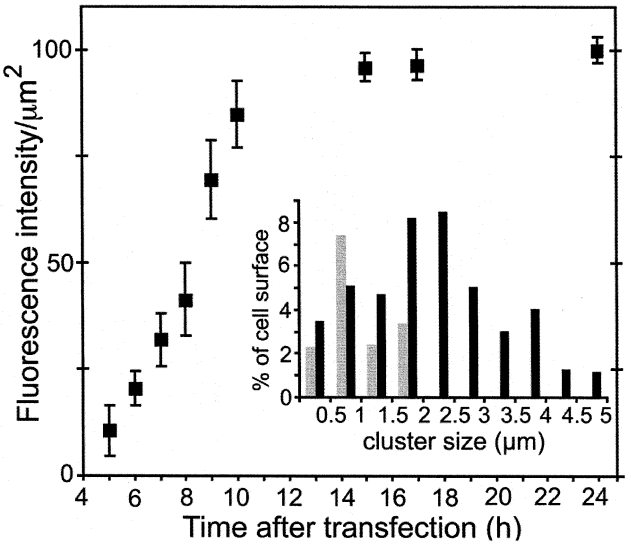

FIGURE 5: Receptor densities on plasma membranes of HEK293 cells at different times after transfection. Cells were transiently transfected with $5HT_3R$ DNA, stained by pulse labeling with a 2 nM solution of GR-rho at the indicated times, and washed with a buffer solution. Fluorescence intensities of the ligand−receptor complexes were measured in a defined area of interest, either in homogeneous nonclustered regions (≤8 h post-transfection) or in clusters (≥9 h post-transfection), and plotted as fluorescence intensity per square micrometer normalized to a value of 100 for the signals obtained in clusters 24 h after transfection. The inset shows the distribution of surface coverage of $5HT_3R$ clusters of different sizes (major axes) on HEK293 cells 9 h (gray bars) and 24 h (black bars) after transfection. Shown are average values obtained from evaluating confocal microscope images of 20 different HEK293 cells stained with a 2 nM GR-flu solution as described in the legend of Figure 3.

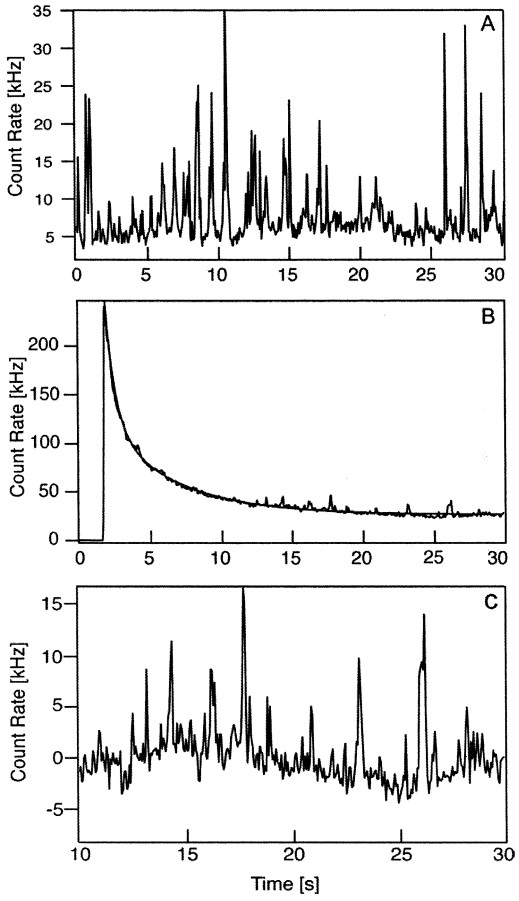

FIGURE 6: Fluorescence correlation spectroscopy on surfaces of HEK293 cells stained with GR-Cy5. (A) Typical fluorescence intensity fluctuations recorded on certain cell surface regions yielded autocorrelation functions (not shown) which could be fitted by three distinct relaxation times corresponding to fluorescent GR-Cy5 ligands (i) diffusing free in bulk extracellular medium, (ii) partitioned unspecifically into the cellular membrane, and (iii) bound specifically to $5HT_3Rs$. (B) Fluorescence intensity trace revealing strong photobleaching at particular sites (different from those in panel A) on the cell membrane. The fluorescence decay was fitted by two exponentials. (C) After the calculated double-exponential curve had been subtracted from the experimental intensity trace in panel B, a flat curve remained showing typical fluctuations as expected for laterally diffusing receptors in a cell membrane. Experimental conditions for the FCS experiment were as follows: a GR-Cy5 concentration in the medium surrounding the cell of 12 nM and a laser power of 0.7 mW.

receptor clusters observed previously by confocal microscopy. The major part of the receptors within the cluster regions is immobile on the time scale of >15 min, whereas a minor part shows lateral diffusion as in the membrane regions surrounding the clusters.

CONCLUSIONS

Recombinant $5HT_3Rs$ on the surface of transiently transfected human embryonic kidney cells were expressed at high density, and the formation of the receptors and their distribution over time were monitored. Radioligand binding assays were fitted by Langmuir isotherms, indicating that only one class of binding sites is present. Due to the high binding affinity and the low off-rate of the fluorescent ligand GR-rho, we were able to stain early expressed receptors with this ligand, and subsequently stain with GR-flu, a spectrally distinguishable fluorescent ligand, receptors expressed later. Thus, it was possible to pulse label the $5HT_3R$ at any time after the appearance on the cell surface and to observe the temporal variation of its distribution on the cell surface by confocal microscopy.

These optical pulse labeling experiments allowed detailed on-line observation of receptor traffic in the plasma membrane of live cells. Receptors were monitored from the beginning of their appearance on the cell surface, during their segregation into clusters, and up to the final movement of these clusters within the cellular membrane. Freshly expressed receptors appear first in the basolateral membrane region of the cell, homogeneously distributed in a relatively narrow, ring-shaped area surrounding the cell base. Continuous integration of newly expressed receptors into this ring-shaped membrane area increases the local receptor concentration. Once a threshold of ~3 000−4 000 receptors/μm^2 is reached, receptor clustering starts basolaterally and then growing receptor clusters move within a time frame of hours toward the apical region of the cell. Individual clusters grow until they reach a size of 1−2 μm when they merge to 3−5 μm large macroclusters on the apical region as indicated by their inhomogeneous fluorescence intensity distribution. During continuous growth of the small individual clusters, the fluorescence intensity of the cluster core increases to a limiting value corresponding to a maximal density of ~13 000 receptors/μm^2. Similar high receptor densities have been observed for the nAchr in receptor clusters in native membranes (*9*) and in two-dimensional crystals (*14*, *15*). The

nAchR is according to its size and function very comparable to the 5-HT_3R (*26*, *29*).

Our own observations (unpublished) and results of others indicated that apical clustering of recombinant $5HT_3$Rs also occurred in several other heterologous cell lines (CHO, N1E115, and COS) from different tissues (*37*, *38*). In all cases, including the one described here, clustering apparently does not require coexpression of recombinant anchoring proteins. This is in striking contrast to the closely related nicotinic acetylcholine and $GABA_A$ receptors, both of which have been reported to cluster only in the presence of rapsyn, an actin-associated protein originating from neuromuscular synapses (*9*, *39*, *40*). Also, a microtubule-associated protein, GABARAP, has been shown to promote GABAA receptor clustering (*41*). A similar behavior is known from the ionotropic glycine receptor, which clusters via interaction with gephyrin, a protein anchored to tubulin (*42*, *43*).

Interestingly, throughout our observation period, the fluorescently labeled $5HT_3$Rs remained located in the plasma membrane of a cell. Using GR-rho as a receptor marker, only faint rhodamine signals were detected within the cytosol, indicating slow receptor internalization. Receptor clustering in the plasma membrane might be responsible for the slow internalization process. A similar case has been reported for heterologously expressed glutamate receptors for which clustering extended its average lifetime in the plasma membrane to ~30 h (*44*).

We do not know whether the clustering of the $5HT_3$Rs in the membranes of the heterologous cells is the result of a concentration-dependent receptor−receptor interaction, a lipid raft-mediated aggregation phenomenon, or both. Specific sequence motifs in the transbilayer regions of membrane proteins have been shown to be important for oligomerization of membrane proteins (*45*) and might be also responsible for the receptor aggregation as found in this work.

Our investigations are of general interest in several respects. First, they demonstrate that it is possible to investigate biomolecular interactions selectively and with the sensitivity to detect single molecular events in a complex biomolecular network of live biological cells. We believe that various in vivo and in vitro labeling strategies in combination with single-molecule spectroscopies and microscopies will in the future play an increasingly important role in elucidating the biomolecular network of live biological cells, a central goal in many announced proteomics projects (*46*, *47*). Second, the finding that recombinant receptors can be expressed in such high concentrations that they cover up to half the cellular surface at a density of ~13 000 receptors/μm^2 opens new sources for the efficient crystallization of membrane proteins.

SUPPORTING INFORMATION AVAILABLE

Results that clearly demonstrate that the 5-HT_3Rs are not internalized but remain on the cell surface in the original orientation under our experimental conditions. This material is available free of charge via the Internet at http://pubs.acs.org.

REFERENCES

1. Stahlberg, H., Fotiadis, D., Scheuring, S., Remingy, H., Braun, T., Mitsuoka, K., Fujiyoshi, Y., and Engel, A. (2001) *FEBS Lett. 504*, 166−172.
2. Kühlbrandt, W., and Gouaux, E. (1999) *Curr. Opin. Struct. Biol. 9*, 445−447.
3. Unger, V. M., Kumar, N. M., Gilula, N. B., and Yeager, M. (1999) *Science 283*, 1176−1180.
4. Ostermeier, C., and Michel, H. (1997) *Curr. Opin. Struct. Biol. 7*, 697−701.
5. Müller, D. J., and Engel, A. (2002) *Methods Cell Biol. 68*, 257−299.
6. Riek, R., Pervushin, K., and Wüthrich, K. (2001) *Trends Biochem. Sci. 25*, 462−468.
7. Cartaud, J., Benedetti, E. L., Cohen, J. B., Meunier, J. C., and Changeux, J. P. (1973) *FEBS Lett. 33*, 109−113.
8. Dupont, Y., Cohen, J. B., and Changeux, J. P. (1974) *FEBS Lett. 40*, 130−133.
9. Ramarao, M. K., and Cohen, J. B. (1998) *Proc. Natl. Acad. Sci. U.S.A. 95*, 4007−4012.
10. Fisher, K. A., and Stoeckenius, W. (1977) *Science 197*, 72−74.
11. Stoeckenius, W., Lozier, R. H., and Bogomolni, R. A. (1978) *Biochim. Biophys. Acta 505*, 215−278.
12. Ahl, P. L. (1993) *Biophys. J. 65*, 563−564.
13. Grigorieff, N., Ceska, T. A., Downing, K., Baldwin, J. M., and Henderson, R. (1996) *J. Mol. Biol. 259*, 393−421.
14. Unwin, N. (1998) *J. Struct. Biol. 121*, 181−190.
15. Miyazawa, A., Fujiyoshi, Y., Stowell, M., and Unwin, N. (1999) *J. Mol. Biol. 288*, 765−786.
16. Palczewski, K., Kumasaka, T., Hori, T., Behnke, C. A., Motoshima, H., Fox, B. A., Le Trong, I., Teller, D. C., Okada, T., Stenkamp, R. E., Yamamoto, M., and Miyano, M. (2000) *Science 289*, 733−734.
17. Grisshammer, R., and Tate, C. G. (1995) *Q. Rev. Biophys. 28*, 315−422.
18. Lundstrom, K. (1997) *Curr. Opin. Biotechnol. 8*, 578−582.
19. Tate, C. G. (2001) *FEBS Lett. 504*, 94−98.
20. Maricq, A. V., Peterson, A. S., Brake, A. J., Myers, R. M., and Julius, D. (1991) *Science 254*, 432−437.
21. Schmid, E. L., Tairi, A. P., Hovius, R., and Vogel, H. (1998) *Anal. Chem. 70*, 1331−1338.
22. Wohland, T., Friedrich, K., Hovius, R., and Vogel, H. (1999) *Biochemistry 38*, 8671−8681.
23. Tairi, A. P., Hovius, R., Pick, H., Blasey, H., Bernard, A., Surprenant, A., Lundstrom, K., and Vogel, H. (1998) *Biochemistry 37*, 15850−15864.
24. Wohland, T., Friedrich-Bénet, K., Pick, H., Preuss, A., Hovius, R., and Vogel, H. (2001) in *Single Molecule Spectroscopy Chemical Physics 67*, pp 195−210, Springer, New York.
25. Vallotton, P., Hovius, R., Pick, H., and Vogel, H. (2001) *ChemBioChem 2*, 205−211.
26. Reeves, D. C., and Lummis, S. C. (2002) *Mol. Membr. Biol. 19*, 11−26.
27. Jackson, M. B., and Yakel, J. L. (1995) *Annu. Rev. Physiol. 57*, 447−468.
28. Hucho, F., and Weise, C. (2001) *Angew. Chem., Int. Ed. Engl. 40*, 3101−3116.
29. Boess, F. G., Beroukhim, R., and Martin, I. L. (1995) *J. Neurochem. 64*, 1401−1405.
30. Jordan, M., Schallhorn, A., and Wurm, F. M. (1996) *Nucleic Acids Res. 24*, 596−601.
31. Schmidt, C., Mayer, M., and Vogel, H. (2000) *Angew. Chem., Int. Ed. 39*, 3137−3140.
32. Barnes, E. M. (2000) *Life Sci. 66*, 1063−1070.
33. Claing, A., Laporte, A. L., Garon, M. G., and Lefkowitz, R. J. (2002) *Prog. Neurobiol. 66*, 61−79.
34. Widengren, J., and Rigler, R. (1998) *Cell. Mol. Biol. (Paris) 44*, 857−879.
35. Schwille, P. (2001) *Cell. Biochem. Biophys. 34*, 383−408.
36. Webb, W. W. (2001) *Appl. Optics 40*, 3969−3983.
37. Mukerji, J., Haghighi, A., and Seguela, P. (1996) *Neurochemistry 66*, 1027−1032.
38. Spier, A. D., Wotherspoon, G., Nayak, S. V., Nichols, R. A., Priestley, J. V., and Lummis, S. C. (1999) *Brain Res. Mol. Brain Res. 67*, 221−230.
39. Froehner, S. C., Luetje, C. W., Scotland, P. B., and Patrick, J. (1990) *Neuron 5*, 403−410.

40. Phillips, W. D., Maimone, M. M., and Merlie, J. P. (1991) *J. Cell Biol*. *115*, 1713−1723.
41. Chen, L., Wang, H., Vicini, S., and Olsen, R. W. (2000) *Proc. Natl. Acad. Sci. U.S.A. 97*, 11557−11562.
42. Prior, P., Schmitt, B., Grenningloh, G., Pribilla, I., Multhaup, G., Beyreuther, K., Maulet, Y., Werner, P., Langosch, D., and Kirsch, J. (1992) *Neuron 8*, 1161−1170.
43. Meyer, G., Kirsch, J., Betz, H., and Langosch, D. (1995) *Neuron 15*, 563−572.
44. Mammen, A. L., Huganir, R. L., and O'Brian, R. J. (1997) *J. Neurosci*. *17*, 7351−7558.
45. Ubarretxena-Belandia, I., and Engelman, D. M. (2001) *Curr. Opin. Struct. Biol. 11*, 370−376.
46. Hovius, R., Vallotton, P., Wohland, T., and Vogel, H. (2000) *Trends Pharmcol. Sci. 21*, 266−273.
47. Keppler, A., Gendreizig, S., Gronemeyer, T., Pick, H., and Johnsson, K. (2003) *Nat. Biotechnol.* (in press).

BI026576D